Multielectrode unipolar voltage mapping and electrogram morphology to identify post-infarct scar geometry: validation by histology

Glashan, C.A.; Tofig, B.J.; Beukers, H.; Tao, Q.; Blom, S.A.; Villadsen, P.R.; ... ; Zeppenfeld, K.

JACC: CLINICAL ELECTROPHYSIOLOGY VOL. 8, NO. 4, 2022

PUBLISHED BY ELSEVIER

VENTRICULAR ARRHYTHMIAS - CATHETER ABLATION

Multielectrode Unipolar Voltage Mapping and Electrogram Morphology to Identify Post-Infarct Scar Geometry

Validation by Histology

Claire A. Glashan, MD,[a] Bawer J. Tofig, MD, PhD,[b] Hans Beukers, MD,[a] Qian Tao, PhD,[c] Sira A. Blom, BSc,[a] Peter R. Villadsen, MD,[b] Thomas R. Lassen, MD,[b] Marta de Riva, MD,[a] Steen B. Kristiansen, MD, PhD,[b] Katja Zeppenfeld, MD, PhD[a]

ABSTRACT

OBJECTIVES This study sought to evaluate the ability of uni- and bipolar electrograms collected with a multielectrode catheter with smaller electrodes to: 1) delineate scar; and 2) determine local scar complexity.

BACKGROUND Early reperfusion results in variable endocardial scar, often overlaid with surviving viable myocardium. Although bipolar voltage (BV) mapping is considered the pillar of substrate-based ablation, the role of unipolar voltage (UV) mapping has not been sufficiently explored. It has been suggested that bipolar electrograms collected with small electrode catheters can better identify complex scar geometries.

METHODS Twelve swine with early reperfusion infarctions were mapped with the 48-electrode OctaRay catheter and a conventional catheter during sinus rhythm. BV electrograms with double components were identified. Transmural ($n = 933$) biopsy specimens corresponding to mapping points were obtained, histologically assessed, and classified by scar geometry.

RESULTS OctaRay UV (UV_{Octa}) and BV (BV_{Octa}) amplitude were associated with the amount of viable myocardium at a given location, with a stronger association for UV_{Octa} ($R^2 = 0.767$ vs 0.473). Cutoff values of 3.7 mV and 1.0 mV could delineate scar (area under the curve: 0.803 and 0.728 for UV_{Octa} and BV_{Octa}, respectively). The morphology of bipolar electrograms collected with the OctaRay catheter more frequently identified areas with 2 layers of surviving myocardium than electrograms collected with the conventional catheter (84% vs 71%).

CONCLUSIONS UV mapping can generate a map to delineate the area of interest when using a multielectrode catheter. Within this area of interest, the morphology of bipolar electrograms can identify areas in which a surviving epicardial layer may overlay a poorly coupled, potentially arrhythmogenic, endocardium.
(J Am Coll Cardiol EP 2022;8:437–449) © 2022 by the American College of Cardiology Foundation.

Myocardial infarction (MI) results in subendocardial scars with variable involvement of the intramural and subepicardial layers. The subendocardium, being exposed to oxygenated blood in the left ventricle (LV), can, to varying degrees, survive the occlusion of the upstream coronary artery. The involvement of the subepicardium is highly variable and dependent on time to reperfusion and pre-existing collaterals.[1,2]

From the [a]Department of Cardiology, Leiden University Medical Center, Leiden, the Netherlands; [b]Department of Cardiology, Aarhus University Hospital, Aarhus, Denmark; and the [c]Laboratorium voor Klinische en Experimentele Beeldverwerking-Division of Image Processing, Department of Radiology, Leiden University Medical Center, Leiden, the Netherlands.
The authors attest they are in compliance with human studies committees and animal welfare regulations of the authors' institutions and Food and Drug Administration guidelines, including patient consent where appropriate. For more information, visit the Author Center.

Manuscript received October 13, 2020; revised manuscript received October 27, 2021, accepted November 17, 2021.

ISSN 2405-500X/$36.00 https://doi.org/10.1016/j.jacep.2021.11.012

JACC: CLINICAL ELECTROPHYSIOLOGY VOL. 8, NO. 4, 2022
APRIL 2022:437–449

ABBREVIATIONS AND ACRONYMS

BV = bipolar voltage

BV_{Conv} = bipolar voltage using conventional catheter

BV_{Octa} = bipolar voltage using the OctaRay catheter

EGM = electrogram

IQR = interquartile range

LV = left ventricle

MI = myocardial infarction

TB = transmural biopsy

UV = unipolar voltage

UV_{Octa} = unipolar voltage using the OctaRay catheter

VM = viable myocardium

VT = ventricular tachycardia

Substrate-based approaches to post-MI ventricular tachycardia (VT) aim to delineate areas with thin layers of surviving myocardium, which are critical to sustain VT. Voltage mapping, in which the amplitude of local electrograms (EGMs) is used as a surrogate for the amount of viable myocardium (VM), has become the pillar of substrate-based ablation and has been shown to be effective in delineating areas of transmural scar.[3] However, in scars in which a substantial layer of subepicardial myocardium survives, the near-field EGM arising from thin endocardium may be obscured by the far-field EGM arising from the epicardium.[4] In this situation, a simple reliance on EGM amplitude can be misleading, and a more detailed examination of the EGM characteristics is needed to distinguish between areas with 2 layers of surviving VM and areas of healthy tissue. It has recently been suggested that EGMs collected using microelectrodes are narrower, thus allowing for better discrimination of multiple components compared to conventional electrodes without requiring pacing maneuvres.[4,5]

The aims of this study were 2-fold: 1) to assess the ability of unipolar voltage (UV) and bipolar voltage (BV) mapping with a novel, multielectrode mapping catheter to delineate areas of scar using the true gold standard for validation: histology; and 2) to determine whether EGMs collected using smaller electrodes are better able to identify areas with 2 layers of surviving VM compared to conventional electrodes.

SEE PAGE 450

METHODS

ANIMAL MODELS. The study was approved by the Danish Animal Experiments Inspectorate (file no. 2017-15-0201-01259) and complied with local institutional guidelines. In domestic Danish swine (76 ± 4 kg), MI was induced by inflating an intravascular balloon placed after the first diagonal branch of the left anterior descending coronary artery for 65 minutes before deflation of the balloon, as previously described.[4,6] After 10 weeks, the animals were brought back to the laboratory for the electrophysiologic procedure.

ELECTROANATOMIC MAPPING AND ABLATION. Endocardial voltage mapping of the LV was performed during stable atrial rate using the OctaRay catheter (Biosense Webster) and the CARTO3 (version 7.0) system. The OctaRay catheter consists of 8 splines, each with 6 electrodes with a width of 0.5 mm and surface area of 0.9 mm^2 (center-to-center spacing: 2 mm) (**Figure 1**). After mapping with the OctaRay, a re-map was made using a conventional mapping catheter (ThermoCool SmartTouch Surround Flow catheter, Biosense Webster) with contact force of ≥9 g (**Figure 1**). UV EGMs were taken against Wilson's central terminal and were filtered at a high-pass filter setting of 2 Hz and a low-pass setting of 240 Hz. BV EGMs were filtered at a high-pass setting of 16 Hz and low-pass setting of 500 Hz.

Subsequently, using the conventional catheter, 3 ablation lesions, remote from the scar areas, were applied and tagged to allow for accurate integration of mapping data with full heart histology.[7]

Sacrifice was performed under general anesthesia with potassium chloride to arrest the heart at the end-diastolic phase, which facilitates accurate ex vivo registration with the electroanatomic maps. The heart was excised, rinsed, and filled with HistOmer[8] to maintain end-diastole dimensions and fixated in 4% formaldehyde (Sigma-Aldrich).

EX VIVO IMAGE INTEGRATION. The fixed heart was sliced into 4.5-mm-thick slices using the HistOtech Quick Slicer Flex.[7] Three-dimensional meshes were created from photographs of the slices, imported into CARTO, and merged with mapping data (**Figure 2,** Supplemental Figure 1).[4,7,9]

HISTOLOGIC ANALYSIS. Transmural biopsy (TB) samples with a width of 10 mm were taken from nonablation OctaRay mapping sites and stained with Picrosirius to visualize histology with collagen staining red and myocardium staining yellow. Biopsy specimens were visually inspected and classified as having no fibrosis, dense scar with only a thin layer of surviving endocardial viable myocardium (1-layer VM), scar throughout the width of the biopsy sample with surviving viable myocardium on both the endocardial side and epicardial side (2-layer VM), or border zone fibrosis (transition from scar to transmural viable myocardium within 1 biopsy specimen) (**Figure 3**). Custom software calculated the wall thickness, percentage of fibrosis, and amount of VM (in square millimeters) in each TB specimen.

EGM PAIRING AND ANALYSIS. All CARTO maps were exported and processed in ParaView version 5.6 (Kitware Inc) with custom-made Python plugins. The collected mapping points were projected onto the CARTO conventional mesh. Each OctaRay point was paired with the closest conventional catheter mapping point. If no conventional point was available

FIGURE 1 Schematic of Catheters Used

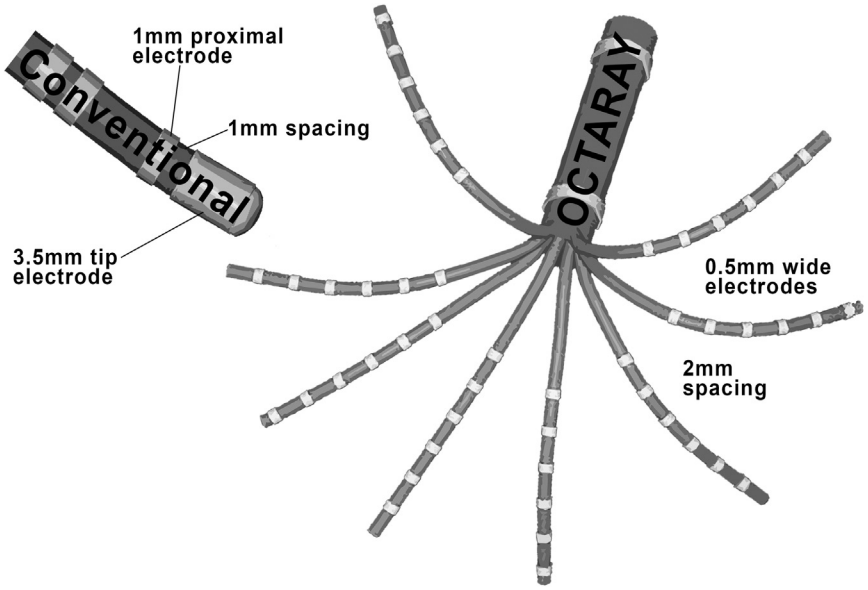

The conventional catheter (ThermoCool SmartTouch Surround Flow catheter, Biosense Webster) consists of a 3.5-mm-tip electrode separated from a 1-mm-ring electrode by 1-mm spacing. The OctaRay catheter consists of 8 splines, each with 6 electrodes with a width of 0.5 mm (0.9-mm^2 surface area) with center-to-center spacing of 2 mm.

within 3 mm, no pair was made. At locations with either 2 layers of VM or border zone fibrosis pattern for which both conventional and OctaRay EGMs were available, the paired BV EGMs were classified as consisting of either 1 component or more than 1 component. Bipolar EGMs consisting of 1 component were further subdivided into near field only or far field only. Far-field components were defined as broad, rounded potentials and near-field as sharp, narrow, high-frequency potentials.[10,11] EGMs with 2 components were classified as having either 2 components distinct in time (2 separated near fields, a near field followed by a far field, or a far field followed by a near field) or 2 overlapping components: a near field occurring within the far-field component (either at the onset or offset of the far-field component) (Figure 4).

STATISTICAL ANALYSIS. Continuous data are reported as mean ± SD, or median (interquartile range [IQR]), as appropriate. Categorical data are expressed as percentages or frequencies. Continuous variables were compared using the unpaired Student's *t*-test or by using linear regression analysis with a mixed-effects model to account for data grouped within 12 animals. Paired nominal data were compared using the McNemar test. Receiver-operating characteristic (ROC) curve analysis was performed to determine the optimal cutoff values, defined as the value maximizing the sum of sensitivity and specificity. Statistical analysis was performed using IBM SPSS, version 25.

RESULTS

ANIMAL MODELS. Twelve swine were included. Coronary occlusion was performed a median of 71 days (range: 70-73 days) before mapping. At the time of mapping, the swine weighed 97 ± 3 kg. A median of 682 (IQR: 608-834) mapping points were collected per LV using the OctaRay catheter. The conventional catheter re-map consisted of a median of 217 (IQR: 192-239) points per LV. Image integration was performed successfully in all swine (Figure 2).

HISTOLOGIC ANALYSIS. A total of 933 TB specimens were taken (median: 67 per heart; IQR: 80-86). Of these, 263 had no pathologicafibrosis.[4,9] These biopsy specimens had a median wall thickness of 11.4 mm

JACC: CLINICAL ELECTROPHYSIOLOGY VOL. 8, NO. 4, 2022
APRIL 2022:437–449

FIGURE 2 **Ex Vivo Image Integration**

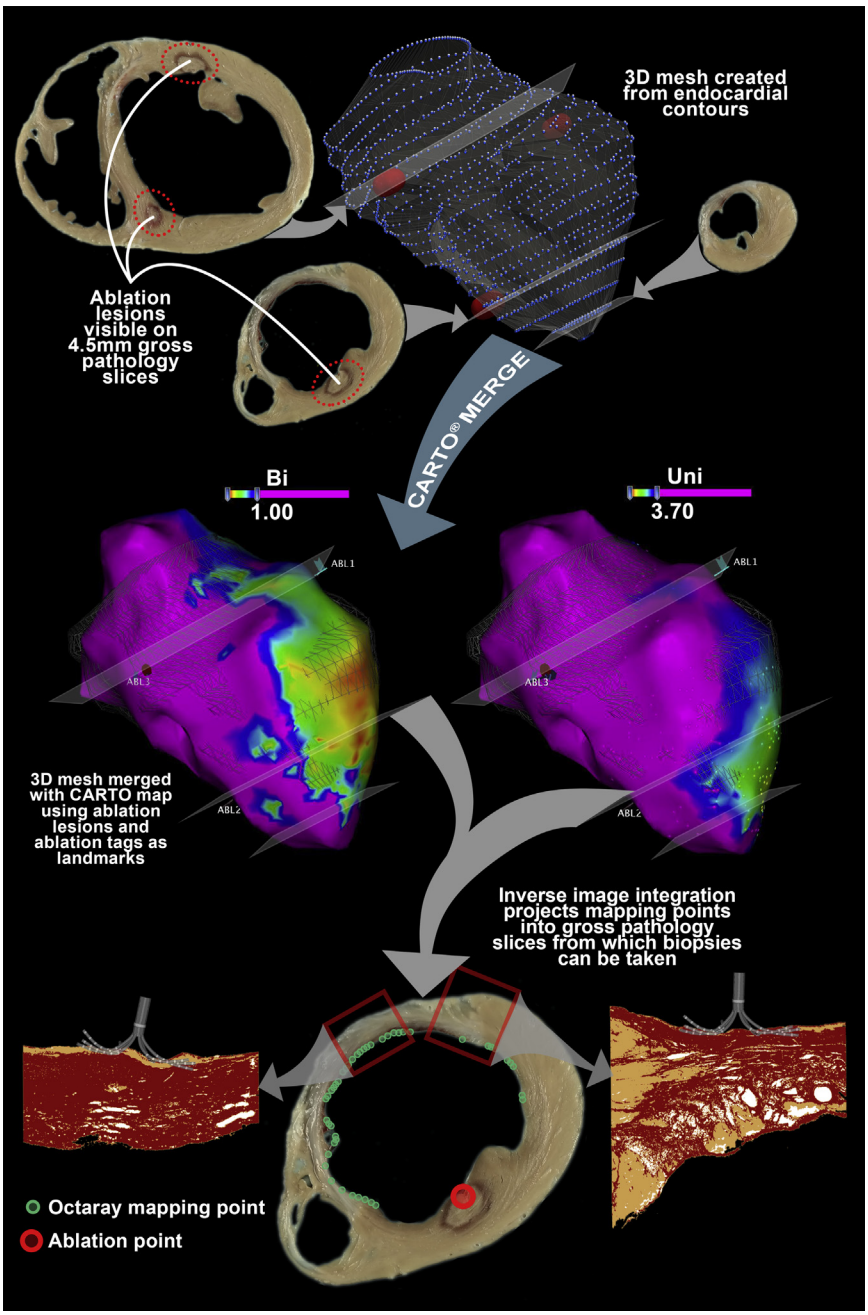

After the mapping and placement of 3 ablation lesions, the heart is excised and fixed in formaldehyde before being sliced into 4.5-mm-thick slices. The 3D-dimensional meshes were drawn from photos of the slices, and these meshes were loaded into CARTO, where they were merged with the in vivo CARTO maps, using the 3 ablation lesions as landmarks. After merging, the data were exported, and in vivo mapping location points were projected onto the pathologic slices. Next, 10-mm-wide TB samples were taken from locations at which mapping data were available and stained with Sirius red for fibrosis (**red** indicates fibrosis, and **yellow** represents viable myocardium). Catheter schematic not to scale. 3D = 3-dimensional; ABL = ablation; Bi = bipolar; Uni = unipolar.

FIGURE 3 Histologic Classification

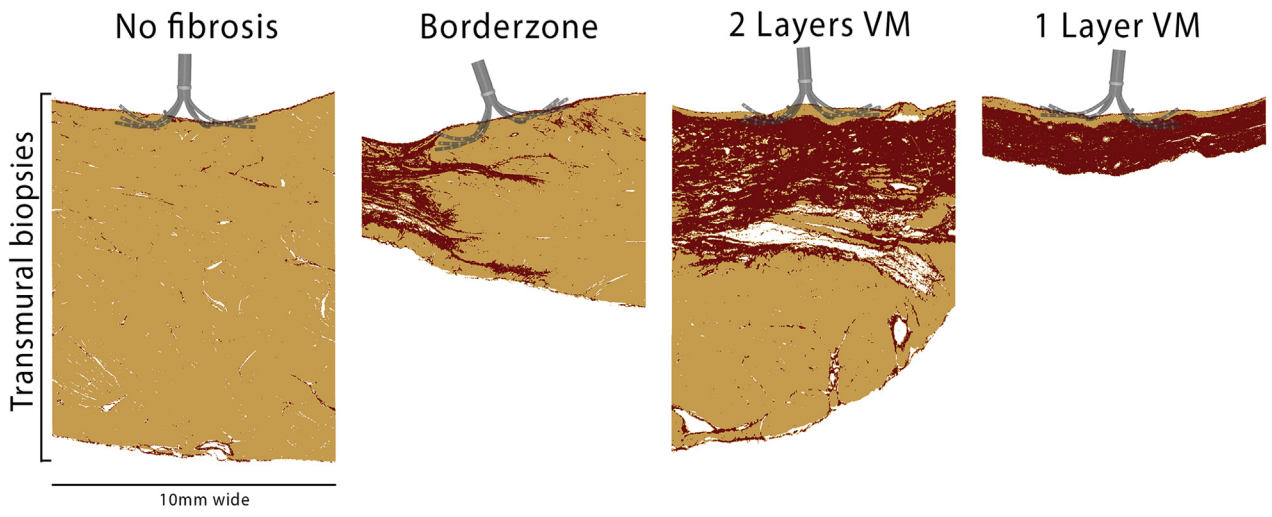

Sirius red staining (**red** indicates fibrosis, and **yellow** represents viable myocardium). No fibrosis: only minimal interstitial fibrosis present. Border zone: transition from some amount of fibrosis to transmural VM within the width of 1 biopsy specimen. Two layers of VM: 1 layer of fibrosis overlying a surviving subendocardial layer of VM with an overlying layer of epicardial myocardium. One layer of VM: 1 layer of fibrosis overlying a surviving subendocardial layer of VM without an overlying layer of epicardial myocardium. Catheter schematic not to scale. VM = viable myocardium.

(IQR: 9.5-13.7), 3.5% fibrosis (IQR: 2.4-4.9), and 108.7 mm^2 VM (IQR: 91-128.4). The 670 biopsy specimens with fibrosis had a median wall thickness of 7.3 mm (IQR: 4.9-10.3), 39.3% fibrosis (IQR: 18-62.4), and 42.3 mm^2 VM (IQR: 17.3-76.5) (Table 1). Of the 670 biopsy specimens, 200 showed a border zone fibrosis pattern, 416 showed 2 layers of VM, and 54 showed 1 layer of VM.

VOLTAGES AND CORRESPONDING HISTOLOGY. Biopsy specimens with no fibrosis generated OctaRay UV (UV_{Octa}) amplitudes with a median of 4.64 mV (IQR: 3.52-6.05). The median OctaRay BV (BV_{Octa}) was 1.59 mV (IQR: 0.74-2.66). Biopsy samples with scar generated UV_{Octa} and BV_{Octa} of 2.66 mV (IQR: 1.79-3.77) and 0.53 mV (IQR: 0.29-1.21), respectively (Table 1).

FIGURE 4 Electrogram Classification

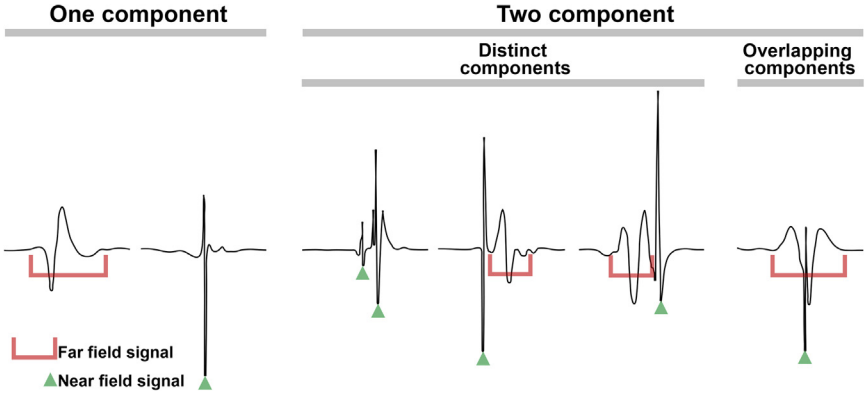

(A) One-component electrograms. Far-field components are defined as broad, rounded potentials and near-field components as sharp, narrow, high-frequency potentials. **(B)** Electrograms with 2 components: 2 distinct near fields, a near field followed by a far field, a far-field followed by a near field, or a near field occurring within the far-field component.

JACC: CLINICAL ELECTROPHYSIOLOGY VOL. 8, NO. 4, 2022
APRIL 2022:437–449

TABLE 1 Histologic and Voltage Parameters in Biopsy Samples With and Without Fibrosis

	No Fibrosis (n = 263)					Fibrosis (n = 670)				
	Percentiles					Percentiles				
	5	25	50	75	95	5	25	50	75	95
Wall thickness, mm	6.9	9.5	11.4	13.7	17.0	2.9	4.9	7.3	10.3	13.7
Fibrosis, %	1.4	2.4	3.5	4.9	8.0	7.4	18.0	39.3	62.4	84.2
Viable myocardium, mm^2	67.2	91.0	108.7	128.4	159.1	5.8	17.3	42.3	76.5	113.2
UV_{Octa}, mV	2.24	3.52	4.64	6.05	8.12	0.94	1.79	2.66	3.77	5.75
BV_{Octa}, mV	0.26	0.74	1.59	2.66	5.76	0.14	0.29	0.53	1.21	3.46

BV_{Octa} = bipolar voltage using the OctaRay catheter; UV_{Octa} = unipolar voltage using the Octaray catheter.

In all biopsy samples, there was a positive relationship between the voltages generated and the amount of VM in the whole TB sample (Figure 5A). For both UV_{Octa} and BV_{Octa}, the association appeared to plateau at higher VM values, in line with previously published results.[4,9] In biopsy specimens with <91 mm^2 VM (25th percentile of biopsy specimens without fibrosis; n = 627), linear regression analysis was performed, and a positive linear relationship was seen for both BV_{Octa} and UV_{Octa}.

Interestingly, the fit for UV_{Octa} ($R^2 = 0.767$; $P < 0.001$) was stronger than for BV_{Octa} ($R^2 = 0.473$; $P < 0.001$), and the same change in VM resulted in a larger change in the UV_{Octa} generated compared to the BV_{Octa} ($\beta = 0.062$ vs 0.024 mV/mm^2).

Similarly, there was a stepwise increase in the voltages generated by biopsy specimens classified as having 1 layer of VM, 2 layers of VM, and border zone and no fibrosis, respectively (Figure 5B). A pairwise analysis showed that there was a significant difference between both the BVs and UVs generated by biopsy specimens with no fibrosis compared to those with border zone fibrosis. The voltages generated by border zone biopsy specimens were also significantly larger than voltages generated at locations with 2 layers of surviving myocardium. Interestingly, although there was a significant difference in the UVs generated at locations with 2 layer of VM compared to locations with 1 layer of VM, this difference was not significant for BV_{Octa}.

Using receiver-operating characteristic analysis, a UV_{Octa} cutoff of 3.7 mV was able to distinguish between locations with no fibrosis and locations with fibrosis with a sensitivity and specificity of 74% (area under the curve: 0.803). A BV_{Octa} cutoff of 1.0 mV (sensitivity: 70%; specificity: 67%; area under the curve: 0.728) was found.

Of the 933 biopsy specimens, 320 were paired to points collected with the conventional catheter (BV_{Conv}). At these 320 locations, a median BV_{Conv} of 0.97 mV (IQR: 0.45-2.0) was recorded. Locations without fibrosis (n = 73) generated a median BV_{Conv} of 1.9 mV (IQR: 1.0-3.3), and locations with fibrosis (n = 247) generated a median BV_{Conv} of 0.77 mV (IQR: 0.38-1.5).

Figure 6 shows a representative example of voltage maps using these cutoff values (UV_{Octa}: 3.7 mV; BV_{Octa}: 1 mV; BV_{Conv}: 1.5 mV). Three locations from which a biopsy specimen was taken without fibrosis were only correctly classified as "normal" all 3 times in the UV_{Octa} map, whereas the BV_{Octa} and BV_{Conv} maps both overestimated the scar size.

BV EGM MORPHOLOGY: CONVENTIONAL VS OctaRay. Of the biopsy samples with 2 layers of surviving VM, 147 biopsy samples had a conventional mapping point located within 3 mm from where the OctaRay data were collected. The classification of the EGMs collected from the OctaRay and conventional catheter are shown in Figure 7. At 88 locations (60%), both conventional and OctaRay EGMs consisted of 2 components, implying that the underlying histologic fibrosis pattern could be inferred from the EGM morphology (1 component arising from the surviving subendocardial layer; a second component arising from the surviving subepicardial layer). Of importance, the OctaRay EGM showed 2 components at 123 locations (84%) with 2 layers, whereas the conventional EGM showed 2 components at only 104 locations (71%) ($P = 0.011$). At 35 locations, 2 components were seen on the OctaRay EGM, whereas only 1 component was seen on the conventional EGM (Figure 8). At 8 locations (5%) neither EGM showed 2 components. In areas that were classified as scar

based on the UV_{Octa} of <3.7 mV but that had a BV_{Octa} of >1 mV, 75% of BV_{Octa} EGMs showed a near field in far-field morphology, 20% showed 2 distinct components, and 5% showed only a far-field signal. Interestingly, none of these EGMs showed only a far-field signal.

Of the biopsy specimens with a border zone pattern of fibrosis, 55 had both conventional and OctaRay mapping data. At these border zone locations, the OctaRay EGM showed 2 components 87% of the time (48/55), whereas the conventional EGM showed 2 components only 69% of the time (38/55) ($P = 0.031$). Interestingly, at 30 of these 55 locations, the UV_{Octa} amplitude was <3.7 mV, and within this subselection, the OctaRay EGM showed 2 components 93% of the time versus 77% of the time for the conventional EGM.

DISCUSSION

This study is the first to couple both the UVs and BVs collected using a novel multielectrode catheter with the true gold standard for fibrosis identification—histology—in an early reperfusion post-MI animal model. Furthermore, we have been able to couple EGMs collected with small electrodes with those collected with a conventional catheter and compare the EGM characteristics at locations with nontransmural scar as identified on histology.

MAIN FINDINGS. 1) Both BV_{Octa} and UV_{Octa} collected using the OctaRay multielectrode catheter are affected by the amount of VM at that location. 2) Cutoff values generated to delineate scar were 3.7 mV for UV_{Octa} and 1.0 mV for BV_{Octa}. Of importance, UV_{Octa} was better able to delineate scar than BV_{Octa} (**Central Illustration**). 3) The morphology of bipolar EGMs collected using the novel multielectrode catheter are more effective in identifying areas with 2 layers of surviving VM than EGMs collected with a conventional catheter.

VOLTAGE MAPPING USING A NOVEL MULTIELECTRODE CATHETER. Using histology as the true gold standard for scar identification, we have coupled the voltage data collected with the OctaRay catheter with the amount of VM underlying the catheter with a high degree of accuracy.[7] Both UV_{Octa} and BV_{Octa} were sensitive to changes in VM occurring at any site throughout the myocardial wall, in line with previously published data.[4,9] As the amount of VM present at a given location increases, so too do the UV_{Octa} and BV_{Octa} generated at that location. In early animal studies, permanent occlusion models gave rise to compact, transmural scars, and in these circumstances, a single cutoff value performs excellently.[12] However, in the current era of early reperfusion, scars are not simple transmural areas of fibrosis. Rather, scars are more heterogeneous, with some areas with only a thin layer of surviving VM on the

FIGURE 5 Relationship Between OctaRay Voltages and Histology

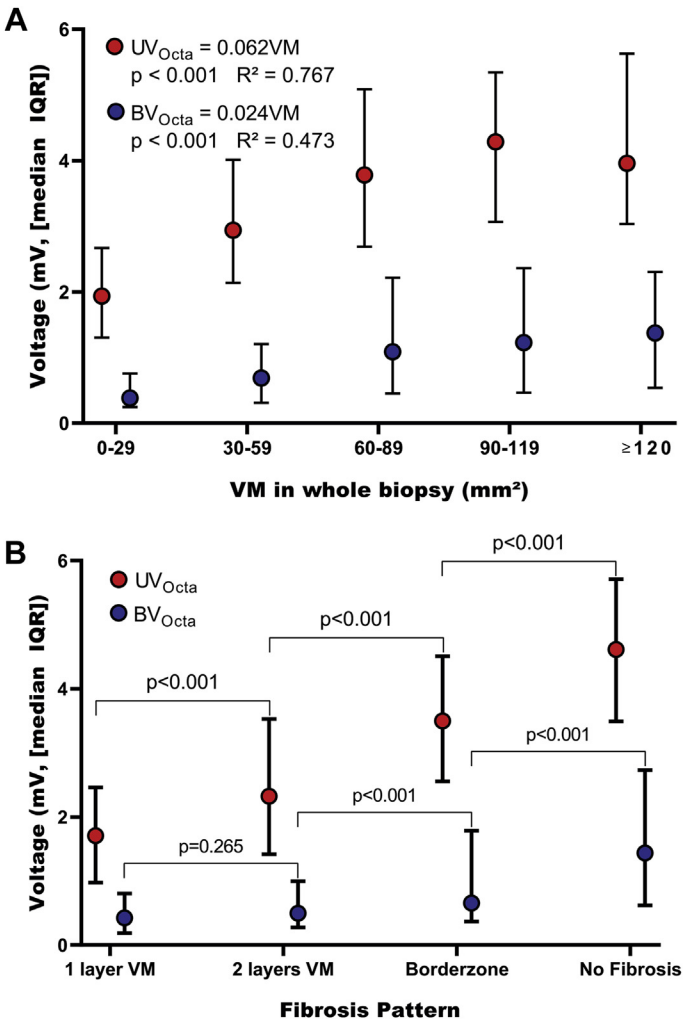

(A) Relationship between voltages and viable myocardium throughout the myocardium. Median ± IQR voltages (UV_{Octa} and BV_{Octa}). **(Top left)** A mixed-models linear regression analysis for biopsy samples with <91 mm^2 VM (25th percentile of biopsy samples without fibrosis; n = 627). **(B)** Voltages generated (median ± IQR) per fibrosis pattern category. *P* values of pairwise Student's *t*-tests. BV_{Octa} = bipolar voltage using the OctaRay catheter; IQR = interquartile range; UV_{Octa} = unipolar voltage using the OctaRay catheter; VM = viable myocardium.

JACC: CLINICAL ELECTROPHYSIOLOGY VOL. 8, NO. 4, 2022
APRIL 2022:437–449

FIGURE 6 Unipolar and Bipolar Voltage Mapping

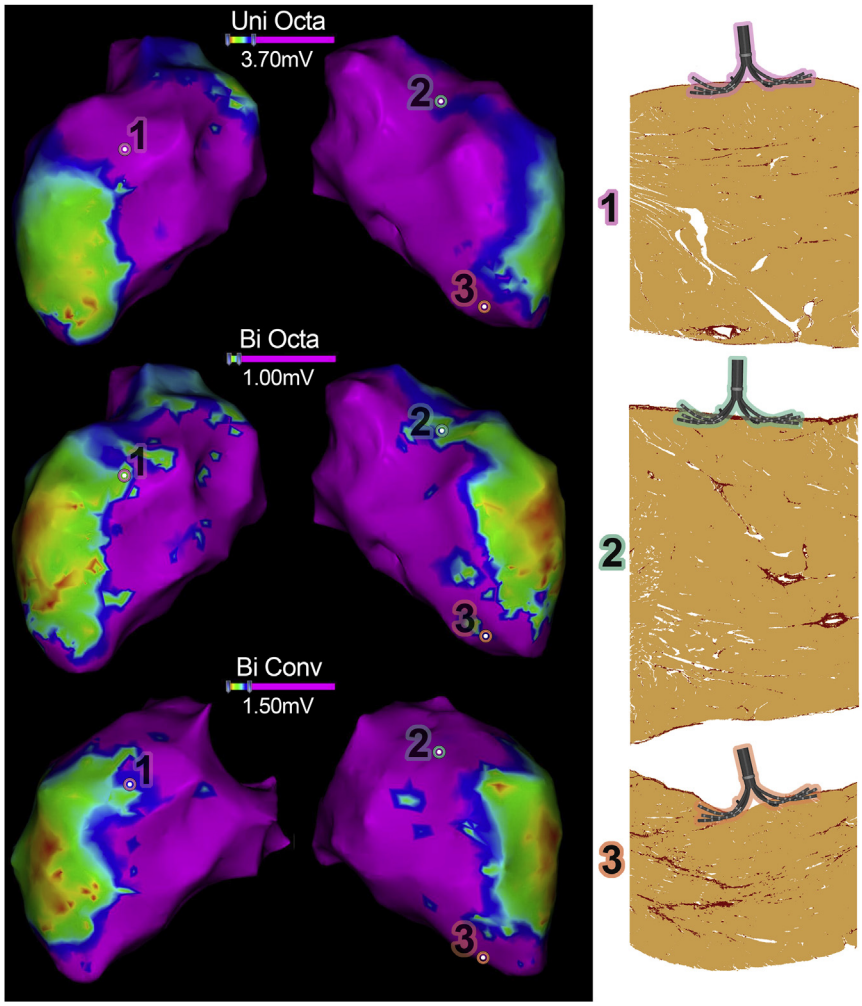

Representative CARTO maps using generated cutoff values (3.7 mV, 1.0 mV, and 1.5 mV for UV_{Octa}, BV_{Octa}, and BV_{Conv}, respectively). Catheter schematic not to scale. BV_{Conv} = bipolar voltage using the conventional catheter; BV_{Octa} = bipolar voltage using the OctaRay catheter; UV_{Octa} = unipolar voltage using the OctaRay catheter.

endocardial surface and other areas in which a layer (of variable thickness) of surviving VM overlays the scar on the epicardial side.[2] Our data suggest that the voltage amplitude can be used to not only identify areas of scar but can also be used to infer the amount of surviving VM overlaying areas of scar. When simply applying—and relying on—a singular cutoff value, some information provided by the voltage map will be lost. Therefore, we must adapt our use and interpretation of voltage mapping accordingly and use a voltage map not as a guide to focus ablation but, rather, as a guide to delineate an area in which more detailed mapping can be performed. With this in mind, the OctaRay catheter, with its 48 electrodes, allows for rapid sinus rhythm mapping, thereby quickly narrowing down the area of interest in which further electroanatomic exploration can be focused.[13]

Surprisingly, the relationship between the voltages generated at a given location and the amount of VM at that location appears stronger for UV_{Octa} than for BV_{Octa} (R^2 = 0.767 vs 0.473). This is not only

FIGURE 7 **EGM Characterization in Biopsy Samples With 2 Layers of Viable Myocardium**

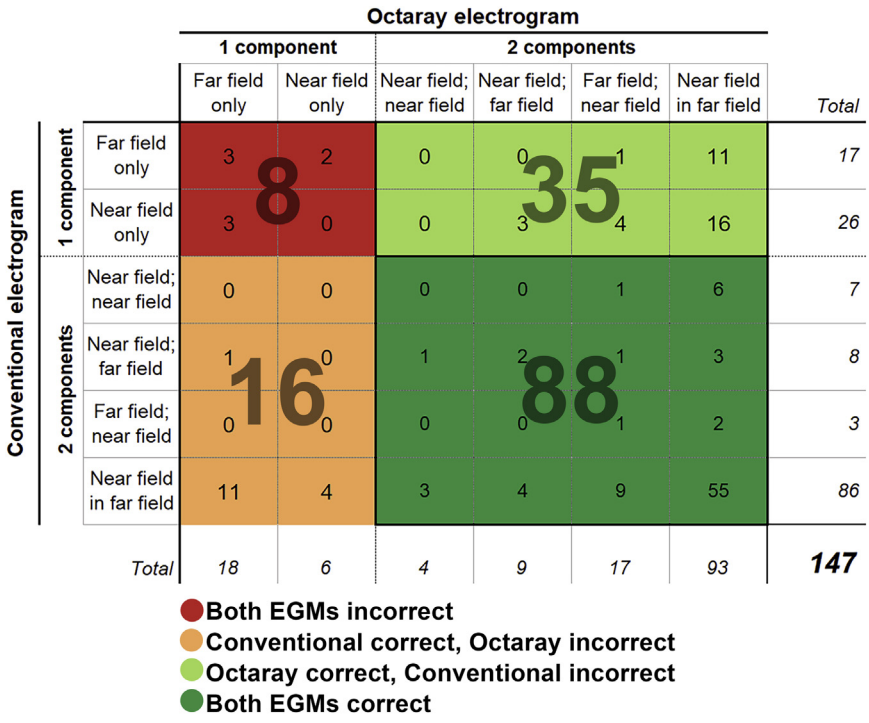

EGM morphology (OctaRay and conventional) at locations with 2 layers of viable myocardium. EGM = electrogram.

academically interesting but practically important. When performing a voltage map to generate a global overview of the scar in a chamber, electrophysiologists will get a more reliable idea of the scar location if they choose to rely on the UV_{Octa} map rather than the BV_{Octa} map (Figure 6). Although initially surprising, the better performance of UV_{Octa} over BV_{Octa} may have a number of explanations. First, as recently shown in a head-to-head comparison between minielectrodes and microelectrodes, BV amplitudes are influenced by the angle of the wavefront propagation relative to the dipole.[14] When comparing the voltage data collected by microelectrodes (using the QDot [Biosense Webster] catheter) at exactly the same location, a different orientation in dipole resulted in an average difference in voltage amplitude of 54%.[14] Unipolar amplitudes, on the other hand, are far less affected by the direction of wavefront propagation.[15] Second, contact force is not measured by the OctaRay catheter. Because BV amplitudes may be more sensitive to a lack of contact than UV amplitudes, the outperformance of UV_{Octa} may be partially explained by this factor.[15] This may also explain the cutoff value generated for BV_{Octa}: 1.0 mV is somewhat lower in amplitude than one would expect from a small and narrow-spaced catheter. Even if the contact force is not known, the global map generated by UV_{Octa} amplitude may still be relied on to demarcate areas without fibrosis, which can then be excluded from further detailed mapping.[13,16]

EGM MORPHOLOGY. We have shown that UV_{Octa} can be used to generate a global view of where scar is located. However, this does not allow one to identify areas within this scar that consist of 2 layers of VM, which may be susceptible to initiating and/or maintaining VT.[17,18] Currently, some centers choose to use a pacing maneuver to unmask areas with poor coupling.[11,19] By further challenging these areas with extrastimulus pacing, areas with functional conduction delay can be identified. It has been shown that

JACC: CLINICAL ELECTROPHYSIOLOGY VOL. 8, NO. 4, 2022
APRIL 2022:437–449

FIGURE 8 **Bipolar Voltage Electrogram Morphology**

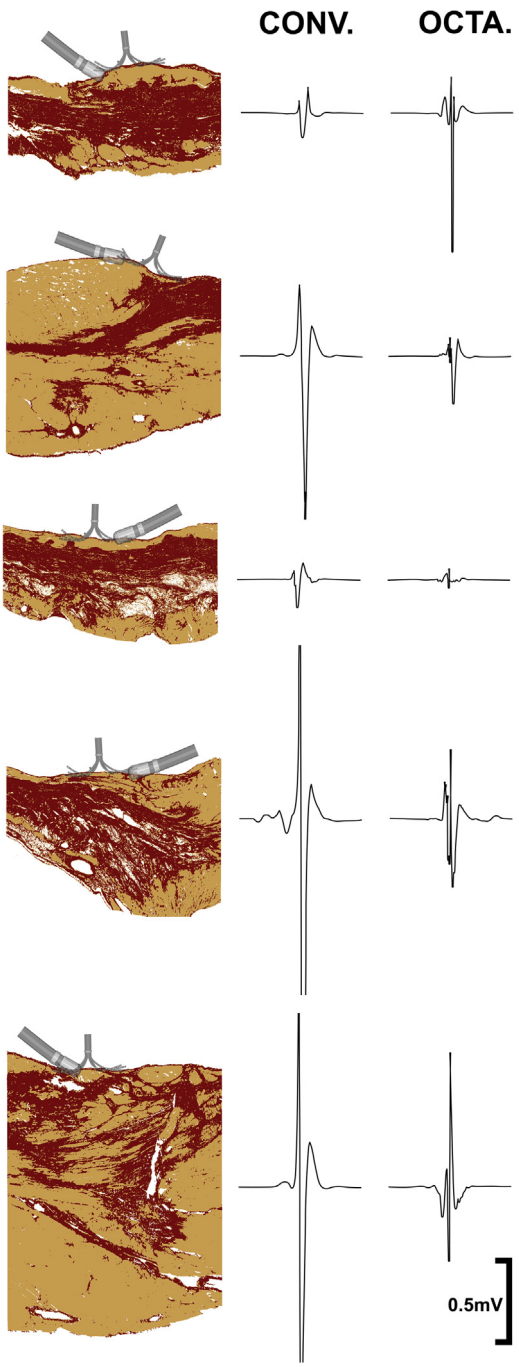

Examples of biopsy specimens with 2 layers of viable myocardium and 1-component conventional (Conv.) electrograms and 2-component OctaRay (OCTA.) electrograms. Catheter schematics not to scale.

targeting these areas improves outcomes in post-MI patients.[11,19] By mapping with smaller electrodes with narrower EGMs, we have shown that we can more easily separate the 2 components that arise from 2 layers of MV, even in sinus rhythm.[4] Furthermore, the high-frequency near-field signal can be more readily distinguished from the rounded far-field signal when both are simultaneously activated (**Central Illustration**). These sites, rapidly identified during sinus rhythm mapping, can then be targeted for additional pacing maneuvers to prove poor coupling and additional conduction delay, which may be related to VT.

Making a sinus rhythm map with the OctaRay catheter provides the electrophysiologist with a plethora of information: the combination of UV_{Octa} amplitudes with BV_{Octa} EGM morphology not only allows for the rapid delineation of scar from healthy tissue but also provides insights into the specific geometry of the fibrosis within the scar area.

STUDY LIMITATIONS. A swine infarct model with an anterior infarct was used in this study; voltages generated by the OctaRay catheter still need to be validated in humans with various scar locations. The cutoff values generated need to be validated in human LV ischemic cardiomyopathy tissue. The histology of 2-dimensional slices corresponding to the mapping points were taken. However, voltage mapping is influenced by the myocardial tissue surrounding the catheter tip in all 3 dimensions, and when merging the mapping data with the gross pathology, minimal translocation may have occurred, resulting in differences in mapped versus histologically analyzed tissue. Although care was taken to ensure good contact, the OctaRay catheter does not measure contact force. Furthermore, the effect of the wavefront was not taken into consideration when performing BV mapping using the OctaRay catheter. Voltage amplitude was measured as peak to peak, which may account for some of the discrepancies seen between BV_{Octa} and UV_{Octa} amplitudes. Although the relationship between voltage mapping and histology has been elucidated, the specific histologic characteristics of VT-related sites have not been explored. Although multicomponent EGMs were correlated with multiple layers of VM, epicardial mapping is needed to definitively identify which component arises from the epicardium and which from the endocardial layer.

CENTRAL ILLUSTRATION **OctaRay Unipolar Voltage Amplitudes and Bipolar Voltage Electrogram Morphology Allow for the Rapid Identification of Complex Postinfarct Scar Geometry**

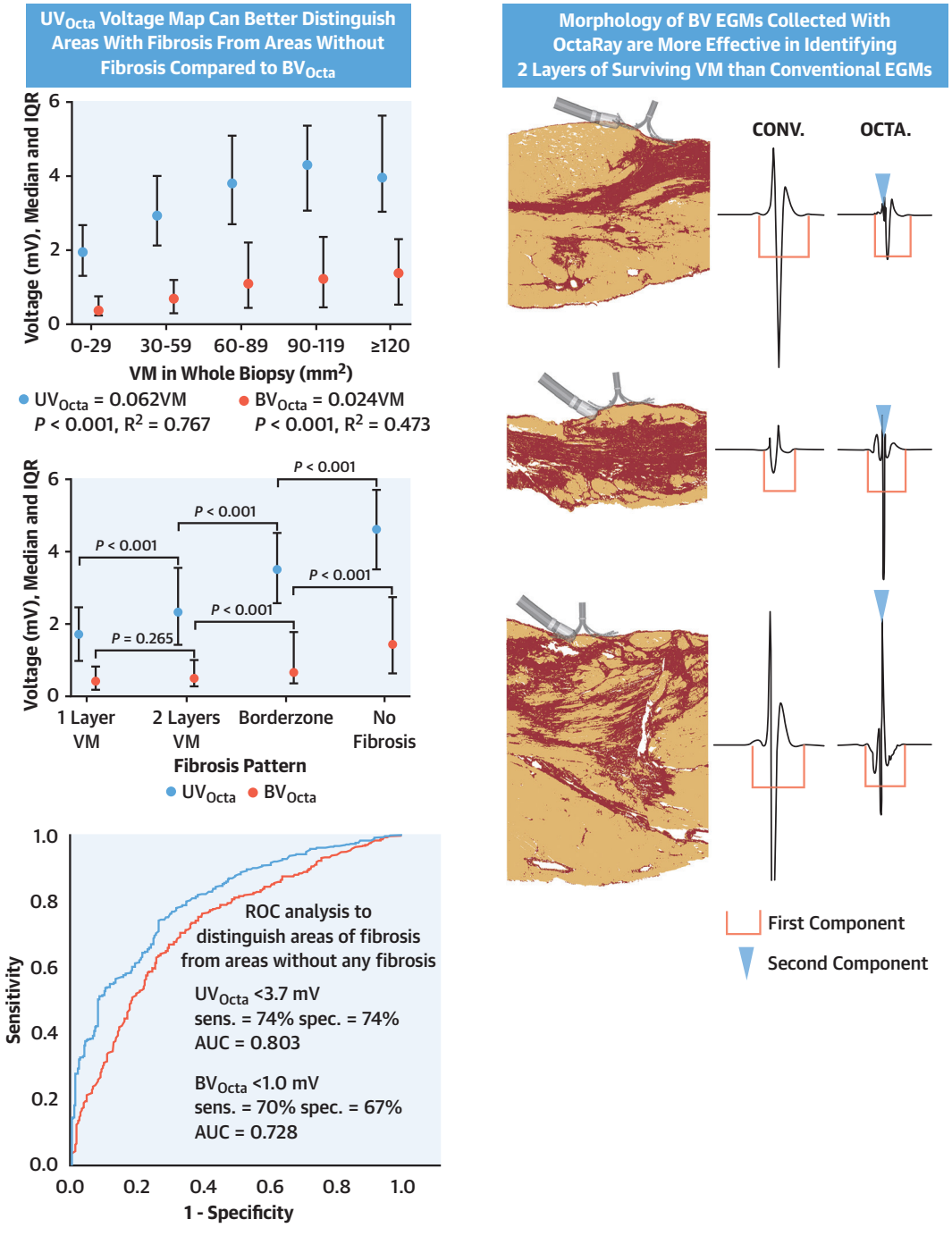

Glashan CA, et al. J Am Coll Cardiol EP. 2022;8(4):437-449.

(Left) The relationship between OctaRay voltages and viable myocardium generated at a given location. The unipolar voltage collected using the OctaRay catheter is better able to distinguish between areas of fibrosis and areas without fibrosis than the OctaRay bipolar voltage, with cutoff values of 3.7 mV and 1.0 mV, respectively. **(Right)** At locations with 2 layers of viable myocardium, bipolar voltage collected using the OctaRay more frequently show double-component electrograms than conventional catheter bipolar voltage electrograms do (84% vs 71%; $P = 0.011$). Catheter schematics not to scale. AUC = area under the curve; BV = bipolar voltage; BV_{Octa} = OctaRay bipolar voltage; CONV. = Conventional; EGMs = electrograms; OCTA. = OctaRay; ROC = receiver-operating characteristic; sens. = sensitivity; spec = specificity; UV_{Octa} = OctaRay unipolar voltage; VM = viable myocardium.

JACC: CLINICAL ELECTROPHYSIOLOGY VOL. 8, NO. 4, 2022
APRIL 2022:437–449

We matched OctaRay points with conventional points within a radius of 3 mm. Although small, even this difference in location may have a significant effect on the histologic substrate underneath the catheter and, as such, on the EGMs generated.

CONCLUSIONS

Using histology as the gold standard in a reperfusion postinfarction model, we have been able to show that UV mapping using the novel OctaRay catheter is better able to delineate areas of scar than BV mapping. Furthermore, bipolar EGMs collected using the OctaRay catheter are better able to identify areas with 2 layers of viable myocardium than bipolar EGMs collected using a conventional catheter.

ACKNOWLEDGMENT The authors thank J.C. Sorensen for graciously allowing us to use HistOmer[8] to embed our tissue.

FUNDING SUPPORT AND AUTHOR DISCLOSURES

This study was partially supported by a research grant from Biosense Webster Inc (a Johnson & Johnson company). Dr Tofig was supported by the Arvid Nilssons Foundation. The authors have reported that they have no relationships relevant to the contents of this paper to disclose.

ADDRESS FOR CORRESPONDENCE: Dr Katja Zeppenfeld, Department of Cardiology (C-05-P), Leiden University Medical Center, PO Box 9600, 2300 RC Leiden, the Netherlands. E-mail: K.Zeppenfeld@lumc.nl.

PERSPECTIVES

COMPETENCY IN MEDICAL KNOWLEDGE: Voltage mapping remains an essential component of VT ablation in ischemic cardiomyopathy. As increasingly smaller electrodes are developed, unipolar voltage mapping becomes a better tool to delineate scar areas. Bipolar electrograms collected using multielectrode catheters are better able to delineate areas of 2 layers of viable myocardium, which may harbor arrhythmic substrate.

TRANSLATIONAL OUTLOOK: These data were collected from an animal model, and the findings need to be validated in humans. Current multielectrode catheters do not have the ability to measure contact force. The development of multielectrode catheters with this feature would be a great advantage.

REFERENCES

1. Piers SR, Wijnmaalen AP, Borleffs CJ, et al. Early reperfusion therapy affects inducibility, cycle length, and occurrence of ventricular tachycardia late after myocardial infarction. *Circ Arrhythm Electrophysiol*. 2011;4:195–201.

2. Wijnmaalen AP, Schalij MJ, von der Thusen JH, Klautz RJ, Zeppenfeld K. Early reperfusion during acute myocardial infarction affects ventricular tachycardia characteristics and the chronic electroanatomic and histological substrate. *Circulation*. 2010;121:1887–1895.

3. Wijnmaalen AP, van der Geest RJ, van Huls van Taxis CF, et al. Head-to-head comparison of contrast-enhanced magnetic resonance imaging and electroanatomical voltage mapping to assess post-infarct scar characteristics in patients with ventricular tachycardias: real-time image integration and reversed registration. *Eur Heart J*. 2011;32:104–114.

4. Glashan CA, Tofig BJ, Tao Q, et al. Multisize electrodes for substrate identification in ischemic cardiomyopathy. *J Am Coll Cardiol EP*. 2019;5(10):1130–1140.

5. Takigawa M, Relan J, Martin R, et al. Detailed analysis of the relation between bipolar electrode spacing and far- and near-field electrograms. *J Am Coll Cardiol EP*. 2019;5(1):66–77.

6. Tofig BJ, Lukac P, Nielsen JM, et al. Radiofrequency ablation lesions in low-, intermediate-, and normal-voltage myocardium: an in vivo study in a porcine heart model. *Europace*. 2019;21:1919–1927.

7. Glashan CA, Tofig BJ, Tao Q, et al. Whole heart histology: a method for the direct integration of histology with electrophysiological and imaging data. *J Am Coll Cardiol EP*. 2020;6(4):461–462.

8. Bjarkam CR, Pedersen M, Sorensen JC. New strategies for embedding, orientation and sectioning of small brain specimens enable direct correlation to MR-images, brain atlases, or use of unbiased stereology. *J Neurosci Methods*. 2001;108:153–159.

9. Glashan CA, Androulakis AFA, Tao Q, et al. Whole human heart histology to validate electroanatomical voltage mapping in patients with non-ischaemic cardiomyopathy and ventricular tachycardia. *Eur Heart J*. 2018;39:2867–2875.

10. Jais P, Maury P, Khairy P, et al. Elimination of local abnormal ventricular activities: a new end point for substrate modification in patients with scar-related ventricular tachycardia. *Circulation*. 2012;125:2184–2196.

11. de Riva M, Naruse Y, Ebert M, et al. Targeting the hidden substrate unmasked by right ventricular extrastimulation improves ventricular tachycardia ablation outcome after myocardial infarction. *J Am Coll Cardiol EP*. 2018;4(3):316–327.

12. Wrobleski D, Houghtaling C, Josephson ME, Ruskin JN, Reddy VY. Use of electrogram characteristics during sinus rhythm to delineate the endocardial scar in a porcine model of healed myocardial infarction. *J Cardiovasc Electrophysiol*. 2003;14:524–529.

13. Cano O, Plaza D, Sauri A, et al. Utility of high density multielectrode mapping during ablation of scar-related ventricular tachycardia. *J Cardiovasc Electrophysiol*. 2017;28:1306–1315.

14. Glashan CA, Beukers HKC, Tofig BJ, et al. Mini-, micro-, and conventional electrodes: an in vivo electrophysiology and ex vivo histology head-to-head comparison. *J Am Coll Cardiol EP*. 2021;7(2):197–205.

15. Anter E, Josephson ME. Bipolar voltage amplitude: what does it really mean? *Heart Rhythm*. 2016;13:326–327.

16. Barkagan M, Sroubek J, Shapira-Daniels A, et al. A novel multielectrode catheter for high-density ventricular mapping: electrogram characterization and utility for scar mapping. *Europace*. 2020;22:440–449.

17. de Bakker JM, van Capelle FJ, Janse MJ, et al. Reentry as a cause of ventricular tachycardia in patients with chronic ischemic heart disease: electrophysiologic and anatomic correlation. *Circulation*. 1988;77:589–606.

18. de Bakker JM, Coronel R, Tasseron S, et al. Ventricular tachycardia in the infarcted, Langendorff-perfused human heart: role of the arrangement of surviving cardiac fibers. *J Am Coll Cardiol*. 1990;15(7):1594–1607.

19. Porta-Sanchez A, Jackson N, Lukac P, et al. Multicenter study of ischemic ventricular tachycardia ablation with decrement-evoked potential (DEEP) mapping with extra stimulus. *J Am Coll Cardiol EP*. 2018;4(3):307–315.

KEY WORDS histology, microelectrodes, myocardial infarction, substrate ablation, swine, ventricular tachycardia

APPENDIX For an expanded Methods section as well as a supplemental figure, please see the online version of this paper.